Materials Science in Semiconductor Processing 75 (2018) 283–287

Contents lists available at ScienceDirect

Materials Science in Semiconductor Processing

journal homepage: www.elsevier.com/locate/mssp

The CO*V* defect in neutron irradiated silicon: An infrared spectroscopy study

D.N. Aliprantis[a], G. Antonaras[a], T. Angeletos[a], E.N. Sgourou[a,b,c], A. Chroneos[b,c,*], C.A. Londos[a]

[a] University of Athens, Solid State Physics Section, Panepistimiopolis Zografos, Athens 157 84, Greece
[b] Faculty of Engineering, Environment and Computing, Coventry University, Priory Street, Coventry CV1 5FB, United Kingdom
[c] Department of Materials, Imperial College, London SW7 2AZ, United Kingdom

ABSTRACT

We report infrared (IR) spectroscopy studies on defects in carbon containing neutron irradiated Czochralski grown silicon (Cz-Si). Prior to irradiation the material was subjected to high temperature treatments (HT) at 1000 °C. Two weak bands at 842 and 852 cm^{-1} were mainly investigated. It was found that their intensity depends on the oxygen and carbon content of Si. Additionally, the bands exhibit an annealing behavior similar to that of the 3942 cm^{-1} optical band of the carbon-oxygen-vacancy (CO*V*) complex, previously reported in electron irradiated Si. Semi-empirical calculations of the local vibration mode (LVM) frequencies of a proposed structure of the CO*V* complex are in very good agreement with our experimental data. These findings led us to assign the pair of bands at 842 and 852 cm^{-1} to the CO*V* defect.

1. Introduction

In the last 60 years, Si prevails as the basic material for most electronic applications [1–5]. The requirement to improve the quality of Si motivates the complete understanding and control of the various imperfections and in particular point defects and their clusters. During the growth procedure various impurities are introduced in the Si lattice, the most dominant being oxygen and carbon. They are unintentionally added in the Si lattice, oxygen at interstitial sites and carbon at substitutional sites. Furthermore, device design and fabrication require processing stages, including thermal treatments and irradiations. These introduce additional defects in the lattice.

As a result of the thermal treatments at high temperatures of Si containing carbon and oxygen, precipitates as well as dislocations, rod-like defects and stacking faults are expected to form [6–9]. Notably, the oxygen precipitation process is accompanied by the emission of Si_I's which aggregate adjacent to the precipitates [9–11]. The stress fields created around the precipitates and generally the extended defects attract Si_I's which are trapped in the interface region (SiO_x/Si) between the oxygen precipitate SiO_x and the Si matrix [9–11]. Thus the interface region is in essence a reservoir of Si_I's and under certain conditions, for instance in the course of irradiation, could act as an additional source of Si_I's. Another factor that affects oxygen precipitation is the presence of carbon in the Si lattice. It has been suggested [9,12–14] that carbon atoms and carbon clusters as well as SiC precipitates in Cz-Si, provide nucleation sites for oxygen precipitation.

As a result of irradiation, defect clusters form. The main defects that form in Cz-Si containing C are the *V*O pair [15,16], as well as the C_iO_i and the C_iC_s pairs [13,17–19]. The latter two pairs form in two stages. Firstly, C_i's are created as a result of the reaction $C_s + Si_I \rightarrow C_i$ which are trapped subsequently by O_i and C_s atoms to form the C_iO_i and the C_iC_s pairs, respectively. For high doses and particularly in the case of neutron irradiations larger complexes form [13,17,18] as for instance $C_i(Si_I)$, $C_iO_i(Si_I)$ and $C_iC_s(Si_I)$ clusters by the addition of Si_I's to the initial C_i, C_iO_i and C_iC_s defects. Besides self-interstitials, vacancies are also expected to be trapped on C-related defects leading to the formation of larger complexes. Thus a weak electronic line at 3942 cm^{-1} (489 meV), detected in electron irradiated Cz-Si contained carbon, was attributed [20–24] to an optical center comprising in its structure at least one C atom, at least one oxygen atom and a vacancy (CO*V*). More specifically, the center was found to be produced in room temperature electron irradiated Si at high doses and it was considered [13] to be a second generation defect consisting of an interstitial carbon atom and a vacancy trapped at an interstitial oxygen atom. Furthermore, it was suggested [13] that the center is produced in the following reactions process: $C_s + (Si_I) \rightarrow C_i$, $C_i + O_i \rightarrow C_iO_i$, $C_iO_i + V \rightarrow$(CO*V*). Other reaction schemes that may be considered [25] for the CO*V* defect production are the following: $C_sO_i + V \rightarrow$ (CO*V*) and $C_i + VO \rightarrow$ (CO*V*). In any case, the concentration of the CO*V* centers is expected to be small and no known LVM signals has been correlated with this line [13,22,23].

The aim of the present study is to investigate the existence of infrared bands that can be correlated with the CO*V* structure. To this end, we have conducted neutron irradiations of C-contained Cz-Si in an

* Corresponding author at: Faculty of Engineering, Environment and Computing, Coventry University, Priory Street, Coventry CV1 5FB, United Kingdom.
E-mail addresses: angelet@phys.uoa.gr (T. Angeletos), alexander.chroneos@imperial.ac.uk (A. Chroneos), hlontos@phys.uoa.gr (C.A. Londos).

https://doi.org/10.1016/j.mssp.2017.11.044
Received 12 October 2017; Received in revised form 27 November 2017; Accepted 29 November 2017

Table 1
Details of the samples used in this work (initial O and C concentrations) as well as the intensities **a** of the 842 and 852 cm^{-1} bands.

Sample	$[O_i]$ (10^{17} cm^{-3})	$[C_s]$ (10^{17} cm^{-3})	$[O_i]_{aft.\ HT}$ (10^{17} cm^{-3})	$[C_s]_{aft.\ HT}$ (10^{17} cm^{-3})	$[O_i]_{aft.irr.}$ (10^{17} cm^{-3})	$[C_s]_{aft.irr.}$ (10^{17} cm^{-3})	a_{842} (cm^{-1}) at 160 °C	a_{852} (cm^{-1}) at 160 °C
M3	7.35	0.51	10.35	0.31	10.39	$< 10^{16}$	0.040	0.028
M5	7.16	1.52	10.32	1.24	10.46	$< 10^{16}$	0.043	0.030
M7	8.63	0.40	13.41	0.38	12.99	$< 10^{16}$	0.051	0.035

attempt to enhance the intensity of weak signals and make possible their detection. Indeed, neutron irradiation causes more substantial damage in the Si lattice and the concentration of defects introduced in the former case is much higher than that in the latter case [26]. Additionally, prior to irradiation, the samples were subjected to thermal treatments at high temperature (HT). The formation of precipitates after these treatments lead to the aggregation of Si_I's in the interface region with the crystal matrix, as we have mentioned above. Accordingly, in the course of irradiation, these Si_I's could be liberated [27] and reacting with C_s atoms it is expected to increase the number of available C_i atoms thus enhancing the possibility of the production of *COV* centers.

2. Experimental details

Three groups of Cz-Si samples (M1, M5, M7) with various oxygen and carbon concentrations were used in this study. Impurities and concentrations are given in Table 1. The samples of ~ 1 × 2 mm dimensions were cut from pre-polished material of ~ 2 mm thickness purchased from MEMC. Samples were initially subjected to thermal treatments at 1000 °C for 5 h. Notably, this temperature is technologically important for Si processes as the diffusion of impurities and oxidation is pronounced impacting the properties of defects including radiation induced defects. After the thermal treatments the samples were irradiated with 5 MeV fast neutrons at fluence of 1 × 10^{17} n cm^{-2}. The irradiations were performed inside a pool of water at ~ 40 °C. For comparison purposes, some samples were irradiated without have being subjected to any previous HT treatment. To eliminate the effect of thermal neutrons, the samples were wrapped in Cd foils and were put in sealed quartz tubes to avoid water contamination. After the irradiation the samples were subjected to 20 min duration isochronal anneals, of ~ 10 °C steps in open furnaces. Inside the furnace the samples were inserted in a quartz cell and all the set in a larger quartz tube to avoid any contamination with the walls of the furnace. The Infrared spectroscopy measurements were carried out after each annealing stage, at room temperature, with a Jasco-IR 700 dispersive spectrometer operating with a spectral resolution of 1 cm^{-1}. The two-phonon absorption was always subtracted by using a reference sample of FZ-Si material of equal thickness. Prior to every measurement the samples were slightly re-polished to remove any oxide layer (SiO_2) which may affect the measurements.

3. Results and discussion

Fig. 1 exhibits segments of the IR spectra for the group M7 samples, one after irradiation without any previous HT (Fig. 1(a)) and one after HT at 1000 °C and then irradiated (Fig. 1(b)), in the frequency range of 800–1050 cm^{-1}. In both samples the well-known bands of the *VO* (828 cm^{-1}), C_iO_i (860 cm^{-1}), $C_iO_i(Si_I)$ (934, 1018 cm^{-1}), $C_i(Si_I)$ (953, 960 cm^{-1}), $C_iC_s(Si_I)$ (987, 993 cm^{-1}) defects are present in the spectra. In addition to these bands, another three at 842, 852 and 883 cm^{-1} are also present in the spectra. They have been also detected previously [28] but were not discussed. This work is focused on studying the behavior and the properties of the two bands at 842 and 852 cm^{-1} which seems to constitute a pair originating from the same defect structure. The bands are very weak and are better presented in the insets of Fig. 1.

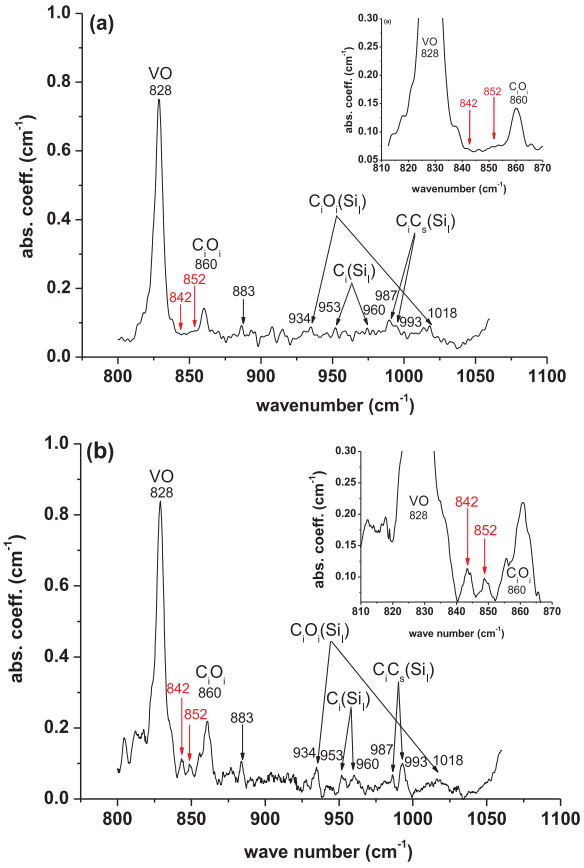

Fig. 1. Segments of the IR spectra of the M7 sample. The two bands at 842 and 852 cm^{-1} are depicted in the inset.

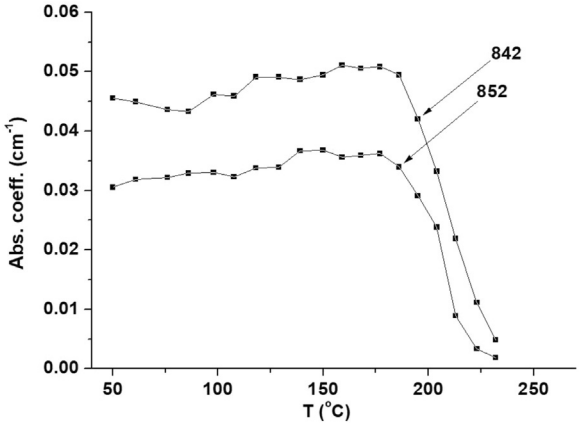

Fig. 2. The annealing behaviors of the 842 and 852 cm^{-1} bands.

Fig. 2 shows the evolution of the 842 and 852 cm^{-1} bands for the HT treated and then neutron irradiated M7 sample. It is easily seen that the annealing behaviors of the two bands are quite similar to that of the 3942 cm^{-1} electronic line (please refer to Fig. 7 of Ref. [20]., showing

the graphical data of the annealing of the 3942 cm^{-1} electronic line).

The next step is to investigate and identify the structure of the defect that gives rise to the 842 and 852 cm^{-1} bands. First, by comparing the intensities of the two bands for the samples M3 and M5 which have about the same oxygen concentration (refer to Table 1) it can be observed that in the sample with the higher carbon concentration the bands are stronger. Similarly, by comparing the intensities of the two bands for the samples M3 and M7 (refer to Table 1) which have about the same carbon concentration it is observed that in the sample with the higher oxygen concentration the bands are stronger. This suggests that the defect contains C and O. Second, due to the neutron irradiation it is reasonable to assume that it also contains vacancies. In general, the concentration of defects introduced by neutron irradiation is much higher than that of electron irradiation [29,30] at the same fluence and therefore the number of vacancies available to participate in the formation of clusters is larger. Third, we observe that the annealing curves of the two bands (refer to Fig. 2) are similar to that of the electronic line 3942 cm^{-1} previously detected (refer to Fig. 7 of Ref. [20]) in electron irradiated, carbon-containing Cz-Si and attributed to a C*OV* defect. Notably, there are numerous examples of different defects in Si which disappear in the same temperature range. However, similar thermal stability between two defects can indicate that there is common origin between the defects and this has to be investigated. In addition, the intensities of the two bands are very weak, indicating that they possibly originate from a second generation defect which is the case for the 3942 cm^{-1} line. It is reasonable, therefore to consider that the bands at 842 and 852 cm^{-1} originate from the same structure, namely the C*OV* defect. Furthermore, we observe that the bands are stronger in the initially HT treated sample. This can be understood as follows. In the course of irradiation of the thermally treated material additional Si_I's are liberated. They interact with C_s atoms leading to the formation of additional C_i atoms that could enhance the formation of C*OV* defects via the reactions $C_s + Si_I \rightarrow C_i$, $C_i + O_i \rightarrow C_iO_i$, $C_iO_i + V \rightarrow COV$ and $C_i + VO \rightarrow COV$ discussed above. Sources of these Si_I's are the oxygen precipitate/Si matrix interface and large extended defects as stacking faults and dislocation dipoles [6,7,31]. In the following further arguments are provided to support the assignment of the bands at 842 and 852 cm^{-1} to the C*OV* defect, by calculating the LVM's of such a structure.

One possible configuration of the structure of the C*OV* complex is that comprising a C_i defect close to a *VO* pair (refer to Fig. 3). Let the frequency of the *VO* defect be Ω_o (835 cm^{-1}) [32]. Apparently, this frequency is modified within the C*OV* structure and becomes ω_o. Similarly, let the frequencies of the C_i defect be Ω_c (922 cm^{-1} and 932 cm^{-1}) [33]. Apparently, these frequencies are modified within the C*OV* complex to ω_c. In the following we calculate the ω_o and ω_c frequencies using a previously reported semi-empirical model [34]. In the C*OV* structure one expects that the silicon atom Si1 (refer to Fig. 3) comes closer to the oxygen atom (in comparison with the unperturbed *VO* defect), because of the tension caused by the interstitial carbon atom of the C_i defect. Therefore, we expect $\omega_o > \Omega_o$. The inverse argument holds for the carbon atom, therefore $\omega_c < \Omega_c$.

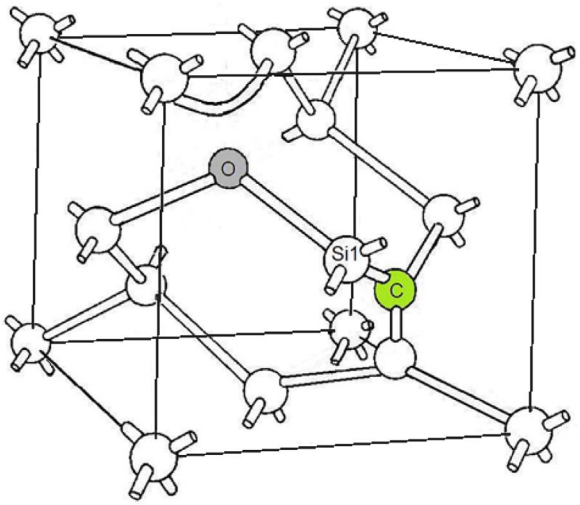

Fig. 3. Suggested structure of the C*OV* defect.

We consider that the oxygen atom of the *VO* defect oscillates near the minimum of a power-law potential:

$$U(r) = 4\varepsilon\left[\left(\frac{\sigma}{r}\right)^4 - \left(\frac{\sigma}{r}\right)^2\right] \tag{1}$$

where ε is the absolute value of the potential $U(r)$ at the equilibrium position r_o of the oxygen atom and $\sigma = \frac{\sqrt{2}}{2} r_o$. This potential is modified by the presence of the C_i defect, within the C*OV* complex in the following way

$$U_+(r) = 4\varepsilon\left[\left(\frac{\sigma}{r}\right)^4 - (1+\lambda_+)\left(\frac{\sigma}{r}\right)^2\right] \tag{2}$$

where λ_+ is a parameter that measures the increase (since $\omega_o > \Omega_o$) in the attractive part of the potential, due to the change of the lattice environment of the oxygen atom.

Similarly, the carbon atom of the C_i defect, oscillates near the minimum of the analogous power-law potential:

$$U'(r) = 4\varepsilon'\left[\left(\frac{\sigma'}{r}\right)^4 - \left(\frac{\sigma'}{r}\right)^2\right] \tag{3}$$

where ε' and σ' are the corresponding parameters for C_i defect. This potential is modified by the presence of the *VO* defect, within the C*OV* complex, in the following way:

$$U_-(r) = 4\varepsilon'\left[\left(\frac{\sigma'}{r}\right)^4 - (1-\lambda_-)\left(\frac{\sigma'}{r}\right)^2\right] \tag{4}$$

where λ_- is a parameter that measures the decrease (since $\omega_c < \Omega_c$) in the attractive part of the potential, due to the change of the lattice environment of the carbon atom. Observe that in relation (4) there is a negative sign before the parameter λ_- because the attractive part of the potential is reduced, since $\omega_c < \Omega_c$. By setting the first derivative of the potential at the equilibrium position equal to zero, by using Eqs. (2) and (4) we find the following expressions for the bond distances:

$$r_+ = \sigma\sqrt{\frac{2}{1+\lambda_+}} \tag{5}$$

$$r_- = \sigma\sqrt{\frac{2}{1-\lambda_-}} \tag{6}$$

Calculating the second derivative at the equilibrium position we find:

$$\left.\frac{d^2U_+}{dr^2}\right|_{r_+} = \frac{4\varepsilon}{\sigma^2}(1+\lambda_+)^3 \tag{7}$$

Since this second derivative equals the force constant, the latter being proportional to the square of the vibrational frequency, we can write:

$$\omega_O = \alpha\Omega_O \tag{8}$$

where

$$\alpha = (1+\lambda_+)^{3/2} \tag{9}$$

Similarly, we find for the carbon atom:

$$\left.\frac{d^2U_-}{dr^2}\right|_{r_-} = \frac{4\varepsilon}{\sigma^2}(1-\lambda_-)^3 \tag{10}$$

$$\omega_C = \beta\Omega_C \tag{11}$$

where

$$\beta = (1 - \lambda_{-})^{3/2} \tag{12}$$

The bond energy [34,35] as a function of metallicity can be written as:

$$E_{bond} = V_2(1 - \alpha_m) \tag{13}$$

where V_2 is the covalent energy and α_m the metallicity [34]. We consider that the bond energy in Eq. (13) comes, in the case of the oxygen atom within the CO*V* defect, from a power-law potential:

$$U_{\zeta}(r) = 4\varepsilon\left[\left(\frac{\sigma}{r}\right)^4 - (1 - \zeta)\left(\frac{\sigma}{r}\right)^2\right] \tag{14}$$

where ζ is a parameter that measures the effect of metallicity [34]. A similar equation holds for the carbon atom within the CO*V* defect. From Eq. (14) we get the following expression at the equilibrium:

$$E_{bond} = \varepsilon(1 - \zeta)^2 \tag{15}$$

By comparing Eqs. (13) and (15) we find:

$$\zeta = 1 - \sqrt{1 - \alpha_m} \tag{16}$$

Metallicity measures [35,36] the metallic character of a covalent bond and its value for Si is $\alpha_m = 0.81$ (refer to Table I of Ref. [35]). However, when impurities are present in the lattice the situation is different since the metallicity of the Si atoms that bond with these impurities is expected to change. An average value $\langle\alpha_m\rangle$ should be considered. For the case of the carbon impurity in Si, the metallicity of Si–C bonds will be taken equal to the average of the metallicity of Si–Si bonds ($\alpha_m = 0.81$) and C–C bonds ($\alpha_m = 0.40$)(Table I of Ref. [34]), that is $(0.81 + 0.40)/2 \approx 0.61$. For the case of the O impurity in Si, Si–O bonds are much less metallic than Si–Si bonds [38] and their contribution to the metallicity will be taken equal to zero. Thus the initial metallicity of the Si atom Si1 (see Fig. 3) in the undisturbed C_i defect is $\langle\alpha_m\rangle_{i,C} = (3 \times 0.81 + 1 \times 0.61)/4 \approx 0.76$, while the initial metallicity of the Si1 atom in the undisturbed *V*O defect is $\langle\alpha_m\rangle_{i,VO} = (3 \times 0.81 + 1 \times 0)/4 \approx 0.61$. The metallicity of Si1 atom finally becomes $\langle\alpha_m\rangle_f = (2 \times 0.81 + 1 \times 0.61 + 1 \times 0)/4 \approx 0.56$ within the C-O-*V* defect. By using Eq. (16) the differences:

$$\zeta_f - \zeta_{i,C} = (1 - \sqrt{1 - 0.56}) - (1 - \sqrt{1 - 0.76}) \approx 0.17 \tag{17}$$

and

$$\zeta_f - \zeta_{i,VO} = (1 - \sqrt{1 - 0.56}) - (1 - \sqrt{1 - 0.61}) \approx 0.04 \tag{18}$$

can be seen as the changes in the attractive part of the potential for the Si1 atom in reference to the C_i and *V*O defects respectively. Considering bond forces as classical two-body forces that obey the law of action and reaction, we shall assume that the relative change of the attractive part of the potential of the C_i defect is equal to the average relative change of the attractive parts of the potentials of its three neighboring Si atoms. Since from these three atoms only the potential of the Si1 is expected to change, the λ_- value could be taken as one third of the $|\zeta_f - \zeta_{i,C}|$ value, i.e., $\lambda_- \approx 0.057$. Similarly, since the oxygen atom in the *V*O defect has two neighboring Si atoms, the λ_O value can be taken as half of the $|\zeta_f - \zeta_{i,VO}|$ value, i.e., $\lambda_+ \approx 0.02$. From Eqs. (8) and (9) substituting the values of $\lambda_+ \approx 0.02$ and $\Omega_o = 835\ \mathrm{cm}^{-1}$, we find the value $\omega_o = 860\ \mathrm{cm}^{-1}$ for the O-related LVM of the CO*V* defect. As for the C-related LVM, using Eq. (11) and (12), substituting the values of $\lambda_- \approx 0.057$ and $\Omega_c = 922\ \mathrm{cm}^{-1}$ or $932\ \mathrm{cm}^{-1}$, we find the values $\omega_c = 844\ \mathrm{cm}^{-1}$ or $853\ \mathrm{cm}^{-1}$ respectively. These values are very close to the experimental values $842\ \mathrm{cm}^{-1}$ and $852\ \mathrm{cm}^{-1}$.

A comment should be made at this point. The C_i defect is not stable at room temperature and begins to migrate below 270 K by thermally activated diffusion [33,37]. Thus the values 922 and $932\ \mathrm{cm}^{-1}$ reported above refer to measurements at 77 K [33]. Accordingly, we used a value for the *V*O center band which also refers to IR measurements made at 77 K [32]. Apparently, by using these values for the C_i and the *V*O defect, the estimated LVMs for the CO*V* defect refer to values at low temperatures. Thus, when we made comparisons with our experimental values of the $842\ \mathrm{cm}^{-1}$ and $852\ \mathrm{cm}^{-1}$ bands recorded at room temperatures, an additional small error is introduced. For instance, the LVM frequency of the *V*O defect is around $830\ \mathrm{cm}^{-1}$ for room temperature measurements [38], instead of $835\ \mathrm{cm}^{-1}$ for low temperature measurements [33]. However, the calculated values for our two bands are very close to the experimental ones allowing for the correlation of the $842\ \mathrm{cm}^{-1}$ and $852\ \mathrm{cm}^{-1}$ bands with the particular CO*V* structure discussed above.

A final comment: Our semiempirical approach on the proposed structure of the CO*V* defect helps us to calculate approximately the relative LVM frequencies. The corresponding values were in agreement with the experimental ones. In future work the CO*V* defect should be investigated using density functional theory calculations (as in previous work [39-41]) to verify the tentatively proposed structure discussed here.

4. Conclusions

We have performed experimental and theoretical studies to investigate the behavior of two bands at $842\ \mathrm{cm}^{-1}$ and $852\ \mathrm{cm}^{-1}$ that emerge in the IR spectra of carbon containing Cz-Si heat treated at 1000 °C and then neutron irradiated. The experimental results indicate that the center responsible for the above two bands contains carbon and oxygen. The annealing curves for the two bands show similar annealing characteristics with a previously reported weak electronic line at $3942\ \mathrm{cm}^{-1}$ (489 MeV) detected in electron irradiated Cz-Si containing carbon and attributed to a carbon-oxygen-vacancy (CO*V*) complex. Since the available amount of vacancies is expected to increase in neutron irradiation, we tentatively assign the $842\ \mathrm{cm}^{-1}$ and $852\ \mathrm{cm}^{-1}$ bands to a CO*V* complex. Semi-empirical calculations gave significant support in this assignment. It was found that the LVMs frequencies of a CO*V* structure comprising a C_i impurity near a *V*O defect are very close to the experimental values.

Acknowledgments

T. Angeletos would like to thank A.S.Onassis Foundation for financial support for his Ph.D. thesis through scholarship (grant No. G ZL 001-1/2015-2016).

References

[1] J. Coutinho, R. Jones, P.R. Briddon, S. Öberg, L.L. Murin, V.P. Markevich, J.L. Lindström, Phys. Rev. B 65 (2001) 014109.
[2] D.J. Backlund, S.K. Estreicher, Phys. Rev. B 77 (2008) 205205.
[3] H. Wang, A. Chroneos, C.A. Londos, E.N. Sgourou, U. Schwingenschlögl, Sci. Rep. 4 (2014) 4909.
[4] A. Chroneos, E.N. Sgourou, C.A. Londos, U. Schwingenschlögl, Appl. Phys. Rev. 2 (2015) 021306.
[5] J. Zhao, P. Dong, K. Yuan, X. Qiu, J. Zhou, J. Zhao, X. Yu, X. Ma, D. Yang, J. Appl. Phys. 122 (2017) 045705.
[6] H. Bender, J. Vanhellemont, T.S. Moss, S. Mahajan (Eds.), iHandbook on Semiconductors, Materials, Properties and Preparations, 3b Elsevier, North-Holland, Amsterdam, 1994, p. 1637.
[7] A. Borghesi, B. Pivac, A. Sassella, A. Stella, J. Appl. Phys. 77 (1995) 4169.
[8] R.C. Newman, J. Phys.: Condens. Matter 12 (2000) R335.
[9] U. Gosele, Mater. Res. Soc. Symp. Proc. 59 (1986) 419.
[10] R.C. Newman, Mater. Res. Soc. Symp. Proc. 104 (1988) 25.
[11] H. Scmalz, J. Vanhellemont, Mat. Res. Soc. Symp. Proc. 262 (1992) 15.
[12] R.C. Newman, Mater. Res. Soc. Symp. Proc. 59 (1986) 403.
[13] G. Davies, R.C. Newman, Handbook on Semiconductors, Materials, Properties and Preparations, 3b Elsevier, North-Holland, Amsterdam, 1994, p. 1557.
[14] W. Scorupa, R.A. Yankov, Mater. Chem. Phys. 44 (1996) 101.
[15] J.W. Corbett, G.D. Watkins, R.S. McDonald, Phys. Rev. A 135 (1964) 1381.
[16] G. Bemski, Phys. Rev. 30 (1959) 1195.
[17] C.A. Londos, M.S. Potsidi, E. Stakakis, Physica B 340–342 (2003) 551.
[18] G. Davies, Mater. Sci. Forum 38–41 (1989) 151.
[19] C.A. Londos, Semicond. Sci. Technol. 5 (1990) 645.
[20] G. Davies, E.C. Lightowlers, M. Stavola, K. Bergman, B. Svensson, Phys. Rev. B 35 (1987) 2755.
[21] G. Davies, E.C. Lightowlers, M. Stavola, K. Bergman, B. Svensson, Mater. Sci. Forum

10–12 (1986) 893.
[22] G. Davies, E.C. Lightowlers, R.C. Newman, A.S. Oates, Semicond. Sci. Technol. 2 (1987) 524.
[23] G. Davies, S. Hayama, S. Hao, B.B. Nielsen, J. Coutinho, M. Sanati, S.K. Estreicher, K.M. Itoh, Phys. Rev. B 71 (2005) 115212.
[24] A.R. Bean, R.C. Newman, R.S. Smith, J. Phys. Chem. Solids 31 (1970) 739.
[25] P.M. Mooney, L.J. Cheg, M. Sulli, J.D. Gerson, J.W. Corbett, Phys. Rev. B 15 (1977) 3836.
[26] N. Fukata, T. Ohori, M. Suezawa, H. Takahashi, J. Appl. Phys. 91 (2002) 5831.
[27] A. Andrianakis, C.A. Londos, A. Misiuk, V.V. Emtsev, G.A. Oganesyan, H. Ohyama, Solid State Phenom. 156–158 (2010) 123.
[28] C.A. Londos, G.D. Antonaras, M.S. Potsidi, D.N. Aliprantis, A. Misiuk, J. Mater. Sci.: Mater. Electron. 18 (2007) 721.
[29] R.C. Newman, D.H.J. Totterdell, J. Phys. C: Solid State Phys. 8 (1975) 3944.
[30] N. Fukata, T. Ohori, M. Suezawa, H. Takahashi, J. Appl. Phys. 91 (2002) 5831.
[31] K. Tempelhoff, K.F. Spiegelberg, R. Gleichmann, D. Wruck, Phys. Stat. Solidi (a) 56 (1979) 213.
[32] A.R. Bean, R.C. Newman, Solid State Commun. 9 (1971) 271.
[33] A.R. Bean, R.C. Newman, Solid State Commun. 8 (1970) 175.
[34] C.A. Londos, N. Sarlis, L.G. Fytros, K. Papastergiou, Phys. Rev. B 53 (1996) 6900.
[35] W. Harrison, Phys. Rev. B 27 (1983) 3592.
[36] S. Pantelides, W. Harisson, Phys. Rev. B 13 (1976) 2667.
[37] A.K. Tipping, R.C. Newman, Semicond. Sci. Technol. 2 (1987) 315.
[38] L.I. Murin, J.L. Linsdstrom, B.G. Svensson, V.P. Markevich, A.R. Peaker, C.A. Londos, Solid State Phenom. 108–109 (2005) 267.
[39] A. Chroneos, C.A. Londos, E.N. Sgourou, J. Appl. Phys. 110 (2011) 093507.
[40] E.N. Sgourou, D. Timerkaeva, C.A. Londos, D. Aliprantis, A. Chroneos, D. Caliste, P. Pochet, J. Appl. Phys. 113 (2013) 113506.
[41] H. Wang, A. Chroneos, C.A. Londos, E.N. Sgourou, U. Schwingenschlögl, Appl. Phys. Lett. 103 (2013) 052101.